Training Sequence Inserted Single-Carrier Transmission Using 2-Step QRM-ML Block Signal Detection

Katsuhiro TEMMA† Tetsuya YAMAMOTO† and Fumiyuki ADACHI‡
Dept. of Communication Engineering, Graduate School of Engineering, Tohoku University
6-6-05 Aza-Aoba, Aramaki, Aoba-ku, Sendai, 980-8579 Japan
†{tenma, yamamoto}@mobile.ecei.tohoku.ac.jp, ‡adachi@ecei.tohoku.ac.jp

***Abstract*—Near maximum likelihood block signal detection using QR decomposition and M-algorithm (QRM-MLBD) can improve a bit error rate (BER) performance of cyclic prefix inserted single-carrier (CP-SC) transmissions. However, it requires a fairly large number *M* of surviving paths in the M-algorithm and leads to very high computational complexity. Replacing the CP by training sequence (TS) was shown to reduce the number of *M*. Another approach to reduce the complexity of QRM-MLBD is to modify the tree structure constructed by QR decomposition for ML detection. Recently, we proposed a 2-step QRM-MLBD which prunes unreliable symbol candidates before tree search by using the minimum mean square error based frequency-domain equalization (MMSE-FDE) output. In this paper, we apply the 2-step QRM-MLBD to TS inserted SC (TS-SC) transmission in order to further reduce the complexity of QRM-MLBD. We show by computer simulation that 2-step QRM-MLBD can reduce the complexity compared to conventional QRM-MLBD while keeping almost the same BER performance.**

Keywords-component; Single-carrier, near maximum likelihood detection, MMSE-FDE, QR decomposition, M-algorithm, training sequence

I. INTRODUCTION

The bit error rate (BER) performance of broadband single-carrier (SC) transmission severely degrades due to strong inter-symbol interference (ISI) [1]. A cyclic prefix inserted SC (CP-SC) block transmission with minimum mean square error based frequency-domain equalization (MMSE-FDE) can improve the BER performance of CP-SC transmission with a low computational complexity [2, 3]. However, a big performance gap from the matched filter (MF) bound [4] still exists due to the presence of the residual ISI after FDE [5].

Near maximum likelihood block signal detection using QR decomposition and M-algorithm (QRM-MLBD) [6] was proposed for CP-SC transmission [7, 8]. It has been shown that QRM-MLBD can significantly improve a BER performance of CP-SC transmission compared to MMSE-FDE. In CP-SC transmission, a fairly large number *M* of surviving paths in the M-algorithm is required to improve the BER performance because the probability of removing the correct path at early stages becomes high. The use of large *M* leads to increased computational complexity. To remedy this problem, the training sequence (TS) inserted SC (TS-SC) transmission [9] can be used [10]. TS is utilized to reduce the probability of removing the correct path at early stages in M-algorithm.

Another approach to reduce the complexity of QRM-MLBD is to modify the tree structure constructed by QR decomposition for ML detection. Recently, we proposed the 2-step QRM-MLBD [11, 12] which prunes unreliable symbol candidates before tree search by using MMSE-FDE output. 2-step QRM-MLBD aims to reduce the number of paths itself in the tree, and therefore the complexity of tree search can be lowered. In this paper, we apply the 2-step QRM-MLBD to TS-SC transmission.

The rest of the paper is organized as follows. Sections II and III present the TS-SC transmission model and 2-step QRM-MLBD, respectively. In Sect. IV, we evaluate by computer simulation the BER performance of TS-SC using 2-step QRM-MLBD and discuss the computational complexity. Section V offers some concluding remarks.

II. TS-SC TRANSMISSION MODEL

The block structure of TS-SC and CP-SC transmission are compared in Fig. 1. For both TS-SC and CP-SC, the number of useful data symbols and guard interval (GI) length are respectively N_c and N_g. The CP which is the copy of last N_g symbols of each block and the TS which is the identical for all blocks are inserted into GI for CP-SC and TS-SC, respectively. The difference between TS-SC and CP-SC is the size of discrete Fourier transform (DFT) to be used at the receiver. The DFT size is N_c symbols for the CP-SC and is N_c+N_g symbols for TS-SC. By including the TS in the DFT block, we can construct the circular property of time-domain channel matrix. Therefore, the frequency-domain channel matrix can be diagonalized and we can apply a one-tap FDE to TS-SC transmission in common with CP-SC transmission.

Figure 2 shows the TS-SC transmission model assumed in this paper. Throughout the paper, the T_s symbol-spaced discrete time representation is used. We assume a frequency-selective fading channel composed of symbol-spaced L distinct propagation paths. The received signal is a cyclic convolution of the transmitted block and the channel impulse response as long as the GI is longer than the maximum channel time delay.

The data symbol block composed of N_c symbols is expressed using the vector form as $\mathbf{d}=[d(0),\ldots,d(N_c-1)]^T$ ($[.]^T$ denotes the transpose operation). The TS of length N_g symbols $\mathbf{u}=[u(0),\ldots,u(N_g-1)]^T$ is appended at the GI placed at the beginning of each block. The block $\mathbf{s}=[s(0),\ldots,s(N_c+N_g-1)]^T$ to be transmitted is expressed using the vector form as

$$\mathbf{s} = [d(0),\ldots,d(N_c-1),u(0),\ldots,u(N_g-1)]^T = [\mathbf{d}^T\mathbf{u}^T]^T. \quad (1)$$

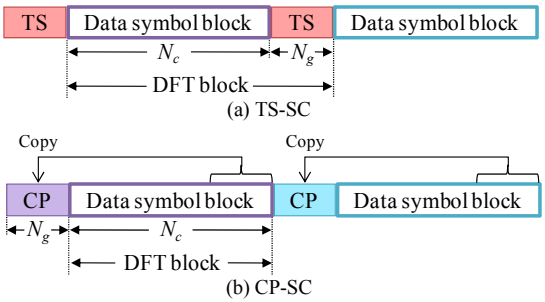

Figure 1. Block structure comparison.

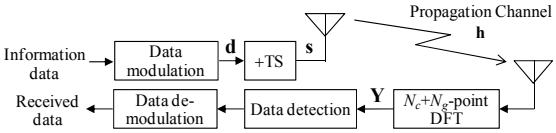

Figure 2. TS-SC transmission model.

At the receiver, N_c+N_g-point DFT is applied to transform the received signal into the frequency-domain signal. The frequency-domain received signal $\mathbf{Y}=[Y(0),\ldots,Y(N_c+N_g-1)]^T$ can be represented as

$$\mathbf{Y}=\sqrt{\frac{2E_s}{T_s}}\mathbf{HFs}+\mathbf{N}, \tag{2}$$

where E_s is the symbol energy. $\mathbf{H}=diag[H(0),\ldots,H(N_c+N_g-1)]$ represents the frequency-domain channel gain matrix and $H(k)=\sum_{l=0}^{L-1}h_l\exp\{-j2\pi k\tau_l/(N_c+N_g)\}$, where h_l and τ_l are the complex-valued path gain with $E[\sum_{l=0}^{L-1}|h_l|^2]=1$ and the time delay of the lth path, respectively. The time delay of each propagation path is assumed to be an integer multiple of the symbol duration. $\mathbf{N}=[N(0),\ldots,N(N_c+N_g-1)]^T$ is the frequency-domain noise vector whose elements are independent zero-mean additive white Gaussian variables having the variance $2N_0/T_s$, N_0 is the one-sided power spectrum density of the additive white Gaussian noise. $\mathbf{F}$ is the $(N_c+N_g)\times(N_c+N_g)$ DFT matrix given by

$$\mathbf{F}=\frac{1}{\sqrt{N_c+N_g}}\begin{bmatrix}1 & 1 & \cdots & 1\\ 1 & e^{-j2\pi\frac{1\times 1}{N_c+N_g}} & \cdots & e^{-j2\pi\frac{1\times(N_c+N_g-1)}{N_c+N_g}}\\ \vdots & \vdots & \ddots & \vdots\\ 1 & e^{-j2\pi\frac{(N_c+N_g-1)\times 1}{N_c+N_g}} & \cdots & e^{-j2\pi\frac{(N_c+N_g-1)\times(N_c+N_g-1)}{N_c+N_g}}\end{bmatrix}. \tag{3}$$

III. 2-STEP QRM-MLBD FOR TS-SC TRANSMISSION

A. Symbol candidate selection using MMSE-FDE output

In the first step of 2-step QRM-MLBD, the symbol candidates to be involved in the path metric computation are selected by performing MMSE-FDE. First, the *a posteriori* probability of each symbol candidate is calculated by using MMSE-FDE output. MMSE-FDE is carried out by multiplying $\mathbf{Y}$ by the MMSE weight matrix $\mathbf{W}$ as [2, 3]

$$\widetilde{\mathbf{S}}=\mathbf{WY}, \tag{4}$$

where

$$\mathbf{Y}=\sqrt{\frac{2E_s}{T_s}}\mathbf{HS}+\mathbf{N}, \tag{5}$$

$$\mathbf{W}=\arg\min_{\mathbf{W}} trE[(\mathbf{WY}-\sqrt{2E_s/T_s}\mathbf{S})(\mathbf{WY}-\sqrt{2E_s/T_s}\mathbf{S})^H]$$
$$=diag\left[\frac{H^*(0)}{|H(0)|^2+\frac{N_0}{E_s}},\cdots,\frac{H^*(N_c+N_g-1)}{|H(N_c+N_g-1)|^2+\frac{N_0}{E_s}}\right], \tag{6}$$

and $\mathbf{S}=\mathbf{Fs}=[S(0),\ldots,S(N_c+N_g-1)]$ is the frequency-domain transmitted signal vector ($[.]^*$ denotes the complex conjugate operation). In order to improve the MMSE-FDE, we introduce the TS cancellation from $\widetilde{\mathbf{S}}=[\widetilde{S}(0),\ldots,\widetilde{S}(N_c+N_g-1)]^T$ as [5]

$$\widetilde{\mathbf{S}}'=\widetilde{\mathbf{S}}-\sqrt{\frac{2E_s}{T_s}}\left\{\widetilde{\mathbf{H}}-\frac{1}{N_c+N_g}tr[\widetilde{\mathbf{H}}]\mathbf{I}_{N_c+N_g}\right\}\mathbf{U}, \tag{7}$$

where $\widetilde{\mathbf{H}}=\mathbf{WH}=diag[\widetilde{H}(0),\ldots,\widetilde{H}(N_c+N_g-1)]^T$ is the frequency-domain channel gain matrix after MMSE-FDE and $\mathbf{I}_J$ is the $J\times J$ unit matrix. $\mathbf{U}=[U(0),\ldots,U(N_c+N_g-1)]^T$ is the frequency-domain TS replica vector represented as

$$\mathbf{U}=\mathbf{F}[\mathbf{0}_{N_c}^T\ \mathbf{u}^T]^T, \tag{8}$$

where $\mathbf{0}_{N_c}$ is the $N_c\times 1$ vector in which all the elements are 0. By applying N_c+N_g-point inverse DFT (IDFT) to $\widetilde{\mathbf{S}}'=[\widetilde{S}'(0),\ldots,\widetilde{S}'(N_c+N_g-1)]^T$, the output of MMSE-FDE $\widetilde{\mathbf{s}}=[\widetilde{s}(0),\ldots,\widetilde{s}(N_c+N_g-1)]^T$ is obtained as

$$\widetilde{\mathbf{s}}=\mathbf{F}^H\widetilde{\mathbf{S}}'=[\widetilde{\mathbf{d}}^T\widetilde{\mathbf{u}}^T]^T, \tag{9}$$

where $\widetilde{\mathbf{d}}=[\widetilde{d}(0),\ldots,\widetilde{d}(N_c-1)]^T$ is the soft decision vector of MMSE-FDE and $\widetilde{\mathbf{u}}=[\widetilde{u}(0),\ldots,\widetilde{u}(N_g-1)]^T$ is the soft output corresponding to TS ($[.]^H$ is the Hermitian transpose operation).

The soft decision output of MMSE-FDE can be written as

$$\widetilde{d}(t)=\sqrt{\frac{2E_s}{T_s}}\left(\frac{1}{N_c+N_g}\sum_{k=0}^{N_c+N_g-1}\widetilde{H}(k)\right)d(t)+\mu_{ISI}(t)+\mu_{noise}(t), \tag{10}$$

where the first, second, and third terms are the desired signal, residual ISI and noise components, respectively. $\widetilde{d}(t)$ is normalized by $A=\sqrt{2E_s/T_s}[\{1/(N_c+N_g)\}\sum_{k=0}^{N_c+N_g-1}\widetilde{H}(k)]$ as

$$\widetilde{d}'(t)=d(t)+\mu'_{ISI}(t)+\mu'_{noise}(t), \tag{11}$$

$$\mu'_{ISI}(t)=\frac{A^{-1}}{N_c+N_g}\sqrt{\frac{2E_s}{T_s}}\sum_{k=0}^{N_c+N_g-1}\{\widetilde{H}(k)-A\}\{\widetilde{S}(k)-U(k)\}\times\exp\left(j2\pi k\frac{t}{N_c+N_g}\right), \tag{12}$$

$$\mu'_{noise}(t)=\frac{A^{-1}}{N_c+N_g}\sum_{k=0}^{N_c+N_g-1}\widetilde{N}(k)\exp\left(j2\pi k\frac{t}{N_c+N_g}\right), \tag{13}$$

with $\widetilde{N}(k)=W(k)N(k)$ representing the noise component after MMSE-FDE. The residual ISI plus noise component

$\mu(t) = \mu'_{ISI}(t) + \mu'_{noise}(t)$ can be treated as a new zero-mean complex Gaussian variable [4] and its variance σ_μ^2 is given by

$$\sigma_\mu^2 = \frac{1}{2} E[|\mu(t)|^2] = \sigma_{ISI}^2 + \sigma_{noise}^2 , \tag{14}$$

$$\sigma_{ISI}^2 = A^{-2} \frac{N_c}{N_c + N_g} \frac{E_s}{T_s} \times \left[\frac{1}{N_c + N_g} \sum_{k=0}^{N_c+N_g-1} \left| \widetilde{H}(k) \right|^2 - \left| \frac{1}{N_c + N_g} \sum_{k=0}^{N_c+N_g-1} \widetilde{H}(k) \right|^2 \right], \tag{15}$$

$$\sigma_{noise}^2 = A^{-2} \frac{1}{N_c + N_g} \frac{N_0}{T_s} \sum_{k=0}^{N_c+N_g-1} |W(k)|^2 . \tag{16}$$

The *a posteriori* probability of each symbol candidate can be calculated by using σ_μ^2.

From Bayes' theorem, when the MMSE-FDE output is obtained, the *a posteriori* probability of a symbol candidate c_i (i=0~X–1, X is the modulation level) can be calculated as

$$P(c_i \mid \widetilde{d}'(t)) = \frac{P(c_i)\, p(\widetilde{d}'(t) \mid c_i)}{p(\widetilde{d}'(t))}, \tag{17}$$

where $P(c_i)$ is the probability that a symbol candidate c_i is transmitted, $p(\widetilde{d}'(t) \mid c_i)$ is the conditional probability density function (pdf) given as

$$p(\widetilde{d}'(t) \mid c_i) = \frac{1}{2\pi\sigma_\mu^2} \exp\left(- \frac{|\widetilde{d}'(t) - c_i|^2}{2\sigma_\mu^2} \right), \tag{18}$$

and $p(\widetilde{d}'(t))$ is the pdf of $\widetilde{d}'(t)$. In this paper, we assume that all the symbol candidates are transmitted with same probability, and therefore, $P(c_i)$=1/X for i=0~X–1. Then, assuming $P(c_i)$=1/X, $P(c_i \mid \widetilde{d}'(t))$ can be calculated as

$$P(c_i \mid \widetilde{d}'(t)) = \frac{P(c_i)\, p(\widetilde{d}'_{n_t}(t) \mid c_i)}{\sum_{j=0}^{X-1} p(\widetilde{d}'(t) \mid c_j) P(c_j)} = \frac{p(\widetilde{d}'(t) \mid c_i)}{\sum_{j=0}^{X-1} p(\widetilde{d}'(t) \mid c_j)} . \tag{19}$$

Next, symbol candidate selection is carried out. Figure 3 shows the process of symbol candidate selection. The symbol candidates are selected in descending order of the *a posteriori* probability and calculate the accumulated *a posteriori* probability. This process continues while the accumulated *a posteriori* probability exceeds the prescribed threshold α.

If α is set too large, only a few symbol candidates are pruned, and therefore the computational complexity of 2-step QRM-MLBD cannot be reduced from QRM-MLBD a lot. However, the use of too small α leads to the transmission performance degradation. In this paper, α is set at each average received E_b/N_0 (=$(E_s/N_0)(1+N_g/N_c)/\log_2 X$) so that the degradation of average symbol error rate (SER) is within the 10% from the average SER of QRM-MLBD with sufficiently large M (e.g. M=16 for 16QAM in TS-SC transmissions) by preliminary computer simulation.

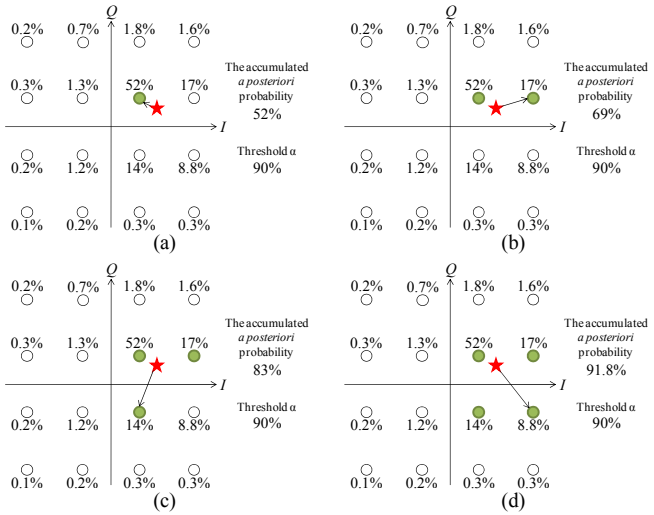

Figure 3. Symbol candidate selection process.

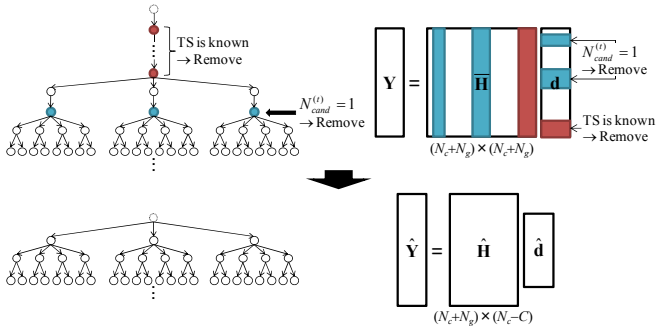

Figure 4. Complexity reduction method for QR decomposition.

B. QRM-MLBD

In the second step, QRM-MLBD is carried out by viewing a concatenation of propagation channel **H** and DFT matrix **F** as an equivalent channel $\overline{\mathbf{H}} = \mathbf{HF}$ in Eq. (2). In this paper, we use the complexity reduction method for QR decomposition using the first step of 2-step QRM-MLBD [12].

The number $N_{cand}^{(t)}$ of remaining symbol candidates associated with $d(t)$ may be limited to only one as shown in Fig. 4. These symbols can be detected by using MMSE-FDE output without tree search, and therefore $d(t)$ with $N_{cand}^{(t)} = 1$ can be removed from received signal by assuming the hard decision results of MMSE-FDE as correct. In this process, the column element of equivalent channel matrix $\overline{\mathbf{H}}$ corresponding to $d(t)$ with $N_{cand}^{(t)} = 1$ can be treated as zero, so the size of channel matrix can be reduced from $(N_c+N_g)\times(N_c+N_g)$ to $(N_c+N_g)\times(N_c+N_g-C)$, where C is the number of $d(t)$ with $N_{cand}^{(t)} = 1$. In addition, TS can also be removed from the received signal as shown in Fig. 4 because TS is known sequence and not related to signal detection. As a result, the size of equivalent channel matrix can be reduced to $(N_c+N_g)\times(N_c-C)$ and the number of complex multiplications required for the QR decomposition is $(N_c+N_g)\times(N_c-C)^2$.

Next, QR decomposition is applied to $(N_c+N_g)\times(N_c-C)$ channel matrix $\hat{\mathbf{H}}$ after applying the method to reduce the complexity of QR decomposition noted above as $\hat{\mathbf{H}} = \hat{\mathbf{Q}}\hat{\mathbf{R}}$,

where $\hat{\mathbf{Q}}$ is the $(N_c+N_g)\times(N_c-C)$ matrix satisfying $\hat{\mathbf{Q}}^H\hat{\mathbf{Q}}=\mathbf{I}_{N_c-C}$ and $\hat{\mathbf{R}}$ is the $(N_c-C)\times(N_c-C)$ upper triangular matrix. Then, multiplying $\hat{\mathbf{Y}}$ which is the received signal vector after removing $d(t)$ with $N_{cand}^{(t)}=1$ and TS by $\hat{\mathbf{Q}}^H$, the transformed received signal $\mathbf{Z}=[Z(0),\ldots,Z(N_c-1-C)]^T$ is obtained as

$$\mathbf{Z}=\hat{\mathbf{Q}}^H\hat{\mathbf{Y}}=\sqrt{\frac{2E_s}{T_s}}\hat{\mathbf{R}}\hat{\mathbf{d}}+\hat{\mathbf{Q}}^H\mathbf{N}$$
$$=\sqrt{\frac{2E_s}{T_s}}\begin{bmatrix}\hat{R}_{0,0} & \cdots & \hat{R}_{0,N_c-1-C}\\ & \ddots & \vdots\\ \mathbf{0} & & \hat{R}_{N_c-1-C,N_c-1-C}\end{bmatrix}\begin{bmatrix}\hat{d}(0)\\ \vdots\\ \hat{d}(N_c-1-C)\end{bmatrix}+\hat{\mathbf{Q}}^H\mathbf{N}, \quad (20)$$

where $\hat{\mathbf{d}}=[\hat{d}(0),\ldots,\hat{d}(N_c-1-C)]^T$ is the $(N_c-C)\times1$ data symbol vector omitting the $d(t)$ with $N_{cand}^{(t)}=1$ from $\mathbf{d}$.

M-algorithm is composed of N_c-C stages. In each stage, the best M paths are selected by comparing the path metrics based on the squared Euclidean distance for all surviving paths and are passed to the next stage. The data detection is carried out by tracing back the path having the smallest path metric at the last stage.

IV. Computer Simulation

We evaluate the average BER performance and computational complexity by computer simulation. We assume 16QAM data modulation, data block size N_c=64, and GI length N_g=16. A partial sequence taken from a Pseudo noise (PN) sequence with repetition period of 127 bits is used as TS. The same data modulation is used for TS and useful data. The channel is assumed to be a frequency-selective block Rayleigh fading channel having symbol-spaced L=16-path uniform power delay profile. Ideal channel estimation is also assumed.

Figure 5 plots the average BER performances of conventional QRM-MLBD and 2-step QRM-MLBD in TS-SC transmissions. Also plotted for comparison is the average BER performance of conventional QRM-MLBD in CP-SC transmissions with M=256. From Fig. 5, we can see that 2-step QRM-MLBD can achieve almost the same BER performance as QRM-MLBD in TS-SC transmission. In order to achieve a close-to-MF bound performance, M=256 is needed for both QRM-MLBD and 2-step QRM-MLBD in CP-SC transmissions [11, 12]. However, only M=16 is enough for both QRM-MLBD and 2-step QRM-MLBD in TS-SC transmissions.

Figure 6 plots the average $N_{cand}^{(t)}$ per stage $(=(1/N_c)\sum_{t=0}^{N_c-1}N_{cand}^{(t)})$ as a function of the average received E_b/N_0 for 2-step QRM-MLBD. Note that for the QRM-MLBD, $N_{cand}^{(t)}$ is always equal to the modulation level X. Figure 7 also plots the average number C of the number of $d(t)$ with $N_{cand}^{(t)}=1$ after symbol candidate selection in the first step. From Figs. 6 and 7, we can see that the average number of $N_{cand}^{(t)}$ can be reduced and many $d(t)$ with $N_{cand}^{(t)}=1$ exist and therefore, the 2-step QRM-MLBD can reduce the computational complexity. As seen from Fig. 6, the value of average $N_{cand}^{(t)}$ (the number of remaining symbol candidates associated with $d(t)$) is largest in a moderate E_b/N_0 region. A possible reason for this is discussed below. In a low and a high E_b/N_0 regions, MMSE-FDE provides the BER performance close to QRM-MLBD although it is much less computationally complex. Therefore, using MMSE-FDE in the first step, the number of symbol candidates for the second step can be made small.

In Table I, the required number of complex multiplications is shown. The TS-SC requires higher complexity to get the frequency-domain signal since DFT is required instead of fast Fourier transform (FFT) when N_c is set to power-of-two value and also requires higher complexity for QR decomposition and multiplication of $\mathbf{Q}^H$ compared to CP-SC. On the other hand, the TS-SC can reduce the required number M of surviving paths in the M-algorithm and therefore, path metric computation can be lowered. 2-step QRM-MLBD additionally requires the computation of MMSE-FDE, cancellation of TS and symbols with $N_{cand}^{(t)}=1$ from received signal and symbol candidate selection. However, the complexity of QR decomposition and the number of symbol candidate to be involved in the path metric computation can be reduced.

Figure 8 shows the average number of complex multiplications per block for achieving close-to-MF bound performance. When the average received E_b/N_0 is less than 8dB, α is set to 0 (i.e., the 2-step soft QRM-MLBD reduces to MMSE-FDE). This is because the performance difference between QRM-MLBD and MMSE-FDE is almost negligible. From Fig. 8, we can see that 2-step QRM-MLBD can reduce the computational complexity compared to QRM-MLBD. The average overall complexity required for TS-SC using 2-step QRM-MLBD reduces to 25% of that required for CP-SC using QRM-MLBD for achieving average BER ≈ 10^{-3} (at the average received E_b/N_0=14dB).

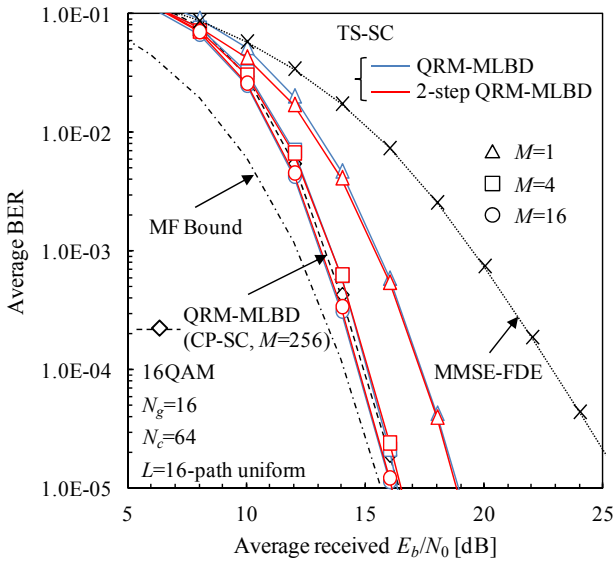

Figure 5. BER performance comparison.

V. CONCLUSIONS

In this paper, we presented 2-step QRM-MLBD for TS-SC. Replacing CP by TS can reduce the required number M of surviving paths in the M-algorithm and pruning unreliable symbol candidates before tree search in the ML detection can reduce the computational complexity of QRM-MLBD. 2-step QRM-MLBD in TS-SC requires only 25% of the average complexity of conventional QRM-MLBD in CP-SC when 16QAM data modulation is used.

TABLE I. THE AVERAGE NUMBER OF COMPLEX MULTIPLICATIONS

	QRM-MLBD		TS-SC using 2-step QRM-MLBD
	CP-SC	TS-SC	
DFT or FFT	$N_c\log_2 N_c$	$(N_c+N_g)^2$	
MMSE-FDE and TS replica cancellation			$(N_c+4)(N_c+N_g)$
IDFT			$(N_c+N_g)^2$
$\overline{\mathbf{H}}$ Computation	N_c^2	$(N_c+N_g)^2$	
σ_μ^2 Computation			$3(N_c+N_g)+1$
Symbol candidate selection			XN_c
Removing the $d(t)$ with $N_{cand}^{(t)}=1$ and TS		$(N_c+N_g)N_c$	$(N_g+C)(N_c+N_g)$
QR decomposition	N_c^3	$(N_c+N_g)N_c^2$	$(N_c+N_g)(N_c-C)^2$
$\mathbf{Z}$ Computation	N_c^2	$(N_c+N_g)N_c$	$(N_c+N_g)(N_c-C)$
Path metric computation	$(N_c+1)X+\sum_{i=2}^{N_c}\left[(i-1+X)\times\min(X^{i-1},M)\right]$		$(N_c+1)E[N_{cand}^{(t)}]+\sum_{i=2}^{N_c-C}\left[(i-1+E[N_{cand}^{(t)}])\times\min(E[N_{cand}^{(t)}]^{i-1},M)\right]$

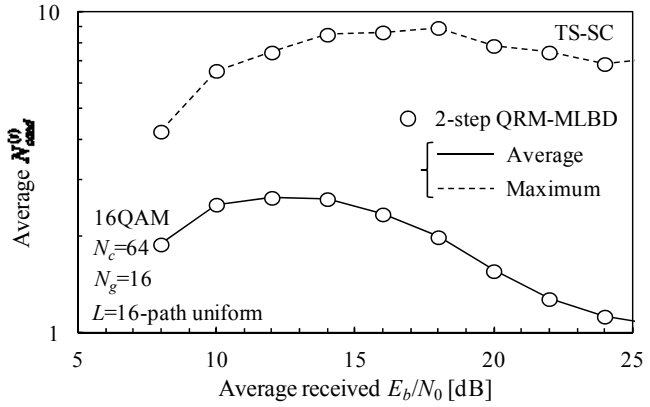

Figure 6. Average $N_{cand}^{(t)}$ per stage.

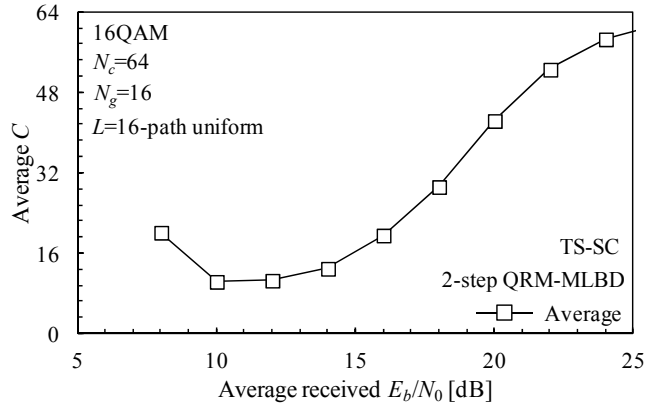

Figure 7. Average C.

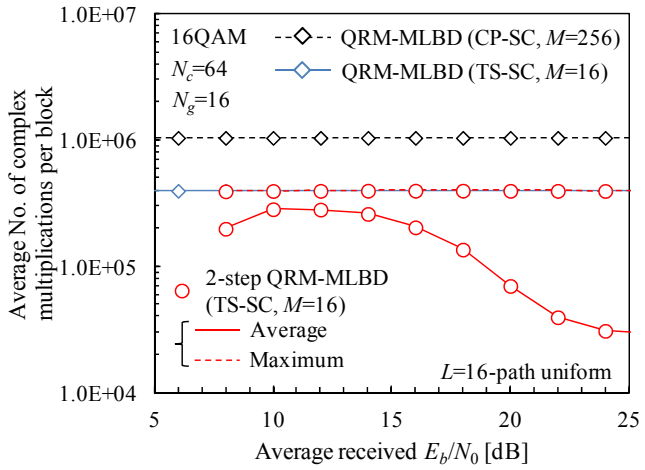

Figure 8. Complexity comparison.

REFERENCES

[1] J. G. Proakis and M. Salehi, *Digital communications*, 5th ed., McGraw-Hill, 2008.

[2] D. Falconer, S. L. Ariyavisitakul, A. Benyamin-Seeyar, and B. Edison, "Frequency domain equalization for single-carrier broadband wireless systems," IEEE Commun. Mag., Vol. 40, No. 4, pp. 58-66, Apr. 2002..

[3] F. Adachi, T. Sao, and T. Itagaki, "Performance of multicode DS-CDMA using frequency domain equalization in a frequency selective fading channel," IEE Electronics Letters, Vol. 39, No.2, pp. 239-241, Jan. 2003.

[4] F. Adachi and K. Takeda, "Bit error rate analysis of DS-CDMA with joint frequency-domain equalization and antenna diversity combining," IEICE Trans. Commun., Vol. E87-B, No. 10, pp.2991-3002, Oct. 2004.

[5] K. Takeda, K. Ishihara, and F. Adachi, "Frequency-domain ICI cancellation with MMSE equalization for DS-CDMA downlink," IEICE Trans. Commun., Vol. E89-B, No. 12, pp. 3335-3343, Dec. 2006.

[6] L. J. Kim and J. Yue, "Joint channel estimation and data detection algorithms for MIMO-OFDM systems," Proc. Thirty-Sixth Asilomar Conference on Signals, System and Computers, pp. 1857-1861, Nov. 2002.

[7] K. Nagatomi, K. Higuchi, and H. Kawai "Complexity reduced MLD based on QR decomposition in OFDM MIMO multiplexing with frequency domain spreading and code multiplexing," Proc. IEEE Wireless Communications and Networking Conference (WCNC 2009), pp. 1-6, Apr. 2009.

[8] T. Yamamoto, K. Takeda, and F. Adachi, "Single-carrier transmission using QRM-MLD with antenna diversity," Proc. The 12th International Symposium on Wireless Personal Multimedia Communications (WPMC 2009), Sept. 2009.

[9] L. Deneire, B. Gyselinckx, and M. Engels, "Training sequence versus cyclic prefix - a new look on single carrier communication," IEEE Commun. Lett., Vol. 5, No. 7, pp. 292-294, July, 2001.

[10] T. Yamamoto, K. Takeda and F. Adachi, "Frequency-domain block signal detection with QRM-MLD for training sequence-aided single-carrier transmission," EURASIP Journal on Advances in Signal Processing, Vol. 2011.

[11] K. Tenma, T. Yamamoto, K. Lee, and F. Adachi, "2-step QRM-MLBD for broadband single-carrier transmission," IEICE Trans. Commun., Vol.E95-B, No.4, pp.1366-1374, Apr. 2012.

[12] K. Temma, T. Yamamoto, and F. Adachi, "Improved 2-step QRM-ML block signal detection for single-carrier transmission," Proc. 2011 IEEE 74th Vehicular Technology Conference (VTC2011-Fall), pp. 1-5, Sep. 2011.